Surface Modification: Advantages, Techniques, and Applications*

K. Natesan

Energy Technology Division
Argonne National Laboratory
9700 South Cass Avenue
Argonne, IL 60439

December 1999

Invited paper presented at the Fifth International Conference on Advances in Surface Engineering, Sao Paulo, Brazil, November 10-13, 1998.

*Work supported by the U.S. Department of Energy, Office of Fossil Energy, Advanced Research and Special Technologies Materials Program, under Contract W–31–109–Eng–38.

DISCLAIMER

Surface Modification: Advantages, Techniques, and Applications

K. Natesan
Energy Technology Division, Argonne National Laboratory
9700 South Cass Avenue, Argonne, IL 60439

Keywords: surface modification, coating method, barrier, sulfur resistance, electrical insulator

Abstract

Adequate performance of materials at elevated temperatures is a potential problem in many systems within the chemical, petroleum, process, and power-generating industries. Degradation of materials occurs because of interaction between the structural material and the exposure environment. These interactions are generally undesired chemical reactions that can lead to accelerated wastage and alter the functional requirements and/or structural integrity of the materials. Therefore, material selection for high-temperature applications must be based not only on a material strength properties but also on resistance to the complex environments prevalent in the anticipated exposure environment.

As plants become larger, the satisfactory performance and reliability of components play a greater role in plant availability and economics. However, system designers are becoming increasingly concerned with finding the least expensive material that will satisfactorily perform the design function for the desired service life. This present paper addresses the benefits of surface modification and identifies several criteria for selection and application of modified surfaces in the power sector. A brief review is presented on potential methods for modification of surfaces, with the emphasis on coatings. In the final section of the paper, several examples address the requirements of different energy systems and surface modification avenues that have been applied to resolve the issues.

Introduction

Over the years, a number of advanced technologies have been developed for the generation of electric power, all of which emphasize high conversion efficiency and stringent environmental compliance. As a result, these technologies require much higher temperatures than are presently in vogue, together with development of barriers between the structural materials/components and the hostile environments prevalent in these systems. Viability of these systems necessitates either the use of alternate advanced materials with inherently superior properties (and significant added expense and less reliability) or modification of the surface regions of the current materials to accommodate the service requirements.

Surface modification in a wider sense includes all types of surface treatments and coatings that result in change in microstructure and composition. There are several methods for modifying the surfaces of structural alloys, dictated by the performance requirements of the alloy in its service environment. One of these approaches is to modify the surface region of engineering alloys via procedures such as ion implantation or sputter deposition of selected elements/compounds accompanied by ion beam mixing, etc. These approaches can create a nonequilibrium alloy chemistry and

microstructures that can impede the transport of reactants from the environment and/or constituents from the substrate. Another approach involves coating of alloy surfaces via techniques such as pack diffusion, low-pressure plasma spraying, electrospark deposition, etc. These avenues generally result in chemical/metallurgical bonding between the deposit and the substrate and provide greater flexibility from the standpoint of composition, microstructure, thickness, etc., of the coating layer. This paper addresses surface modification issues and discusses the advantages, approaches to modify the surfaces with emphasis on coatings, and several applications of interest in advanced energy systems.

Surface modification or coatings can have one or more of the following objectives:

2 Functional need. This means that without the coating, the function of the component cannot be met in service. Some of the examples in this category are thermal-barrier coatings in gas turbines, sulfur-resistant coatings in coal-fired systems, metal-chloride-resistant coatings in waste-to-energy systems, and electrically insulating coatings for liquid-metal blankets in fusion devices.

3 Minimize material wastage. Most of the corrosion-, erosion-, and wear-resistant coatings are used to reduce component degradation with a resultant increase in lifetime.

4 Minimize spallation and downstream erosion. This depicts a situation in which the spallation itself is not of significant consequence, but erosion induced at downstream locations by the material spalled upstream is of concern. An example is oxide exfoliation in steam systems, which can lead to erosion of steam turbines.

5 Minimize material/component cost. This objective is widely justified by application of a relatively expensive surface layer to minimize wastage of otherwise degradable components. The approach can result in substantial cost savings because expensive monolithic material is not used for structures.

The decision to use surface modification or a coating is based on several technical and economic factors, some of which are listed in Table 1.

Surface Modification/Coating Approaches

Coatings can be classified in several ways. Based on the mechanism of the coating process, they can be categorized as an overlay or a diffusion coating. In the overlay coatings, the desired material is placed on a substrate by techniques such as physical vapor deposition (PVD), flame, arc or plasma thermal-spraying, etc. The coating in these cases has a mechanical bond with the substrate, without much diffusion of the coating constituents into the substrate. In diffusion coatings, the coating material generally forms a chemical/metallurgical bond with the substrate. Methods for these coatings generally require high temperatures and include chemical vapor deposition (CVD), pack diffusion, hot dipping, and laser treatments.

Physical Vapor Deposition

These use vaporization of coating constituents from a source and subsequent deposition onto a substrate alloy. Several means for vaporization, such as thermal/chemical, electron beam, plasma, and arc, have been used. Even though PVD is a viable procedure for coating applications, poor adhesion of

the coating to the substrate can be detrimental to coating performance. However, several coatings developed by PVD have been examined for their functional properties, corrosion resistance, and protection of the underlying alloy for service in several energy technologies. One drawback of the PVD technique is that the coating is achieved by line-of-sight application, which limits the shapes of objects that can be coated. Furthermore, the process requires a vacuum system, which restricts the size of the components to be coated.

Sputter Deposited Coatings

In the sputtering process, atoms are removed from a target material by incident energetic ions. Momentum transfer from the energetic ions leads to displacement of atoms in the target material; some of the target atoms escape from the surface and their flight paths can be controlled to develop a film of the target material on a substrate. Typical sputter yields are in 0.1-3 atoms/ion for ion energies up to 1,000 eV. Films of complex chemistries can be prepared by simultaneous sputtering from more than one target material. Functionally graded layers can be developed by sequential sputtering of different target materials. A wide range of materials, including metals, alloys, metal oxides, carbides, and cermets, have been sputter-deposited for a variety of applications.

Because high sputtering yield requires that the target be bombarded having particles with sufficient momentum, argon or other noble gases are generally ionized in a discharge. Magnetrons are widely used because their high ion current densities generally provide higher deposition rates. Radio-frequency sputtering at low gas pressures has been used widely to sputter-deposit several materials. Furthermore, reactive sputtering has been used to deposit compounds such as Al_2O_3, AlN, TiO_2, TiN, etc., by controlling the reaction of sputtered atoms of Al or Ti with O or N in the surrounding environment before depositing onto the substrate.

Pack Diffusion Coatings

In pack diffusion, the component to be coated is fully immersed in a powder mixture of a coating element, an activator, and an inert material. The pack and the component are heated to between 750 and 1100°C for 4-24 hr in a protective atmosphere. This coating process is fairly simple and inexpensive, and large components can be coated with relative ease. However, the pack process lends itself to only simple coating compositions, generally of a single element, primarily because of thermodynamic limitations on transfer of different elements under the same temperature and activator conditions. Attempts have been made to coat two elements simultaneously, such as Al and Cr, Al and Si, or Cr and Si, and the performance of these coatings in complex service environments needs to be evaluated. One drawback is that during the coating process, the component to be coated is exposed to temperatures much higher than the service temperature and this can alter the microstructural and mechanical properties of the base material.

Electrospark Deposition (ESD) Coatings

The ESD process is a microwelding technique that uses short-duration, high-current electrical pulses to deposit an electrode material on a metallic substrate. A principal advantage of ESD is that the coatings are fused to a metal surface with a low heat input while the bulk substrate material remains at ambient temperature. This eliminates thermal distortions or changes in the metallurgical structure of the substrate. Because the coating is alloyed with the surface, i.e., metallurgically bonded, it is inherently

more resistant to damage and spalling than the mechanically bonded coatings produced by most other low-heat-input processes (such as detonation-gun, plasma-spray, and electrochemical plating).

Chemical Vapor Deposition

In CVD process, a reactant atmosphere is fed into the processing chamber, where it decomposes at the surface of the component material, liberating one material for absorption or accumulation on the component surface. The second material is released in gas form and is removed from the processing environment along with the excess of the unreacted input gas. Reactant atmospheres generally involve chlorides, fluorides, bromides, iodides, hydrides, carbonyls, etc. Since the process involves decomposition/reaction, the process temperature is generally >800°C. A derivative of conventional CVD is plasma-assisted CVD, in which the ionized gas in the vicinity of workpiece is used to enhance deposition.

Plasma Spray Coatings

In a conventional plasma spray process, the coating material in powder form is melted in a plasma arc and propelled onto the target surface to form a coating. The method is amenable to formation of coatings of complex compositions and large thicknesses, but whose porosities are generally high. In addition, poor adherence of the coating to the substrate alloy can lead to spalling of the coating, especially under thermal-cycling conditions. Vacuum or low-pressure plasma spray, in which high particle and gas velocities are achieved, has been used to develop coatings with better corrosion resistance than those developed by conventional plasma spray. Interaction between the coating constituents and the underlying alloy elements is generally minimal, and the coating, for all practical purposes, is similar to an overlay coating. However, the size limitation on the vacuum chamber makes coating of large components using this technique virtually impossible. Plasma spraying is widely applied to develop "thermal barrier" coatings for gas turbines, in which a coating with low thermal conductivity is used to thermally shield the blade material from hot gases. A bond coat of MCrAlY is applied to the component by either the PVD, pack process, or plasma spray technique. Subsequently, a ceramic coating, (usually Y_2O_3-stabilized ZrO_2) is applied to the bond coat by the air plasma spray technique.

Thermal Spray Coatings

This approach has been considered for a wide range of industrial applications because it is amenable to field usage; can be tailored to mitigate degradation processes such as corrosion, erosion, wear, etc.; and can be used to repair and restore worn components. The process is flexible in that any metallic or ceramic material can be applied as long as they do not decompose at elevated temperatures of application. In use, the spray material in the form of fine powder or wire is heated to a near molten state and then rapidly accelerated to strike the component surface to be coated. Upon impact, the particles form a splat that cools rapidly and adheres to the component surface. A thicker coating is achieved by continued application of the powder to build up the splats. One major drawback of this technique is the presence of varying degrees of porosity, both isolated and interconnecting, in the multiple splats of the coating thickness. In some instances, the coatings require a postspray densification treatment to reduce the porosity, especially at temperatures much above the service temperatures of the components.

Applications of Coatings

Electrical Insulating Coating for a Fusion Blanket System

The blanket system is one of the most important components in a fusion reactor because it has a major impact on both the economics and safety of fusion energy. The primary functions of the blanket in a deuterium/tritium-fueled fusion reactor are to convert the fusion energy into sensible heat and to breed tritium for the fuel cycle. The liquid-metal blanket concept requires an electrically insulating coating on the first-wall structural material to minimize the magnetohydrodynamic (MHD) pressure drop that occurs during the flow of a electrically conducting liquid metal in a magnetic field. If the flow direction is perpendicular to the field, a potential difference across the duct is induced in the liquid metal. This can cause a high electrical current flow if the potential difference is short-circuited by the duct walls. An electrical current flowing perpendicular to a magnetic field results in a mechanical force that leads to MHD pressure drop.[1] It has been shown that even thin conducting walls would lead to a high pressure drop under the conditions of the fusion blanket; for example, the pressure drop in a poloidal duct in an inboard blanket segment would reach 8.6 MPa if the conducting liner is 0.1 mm thick.[2] This unacceptably high pressure drop shows the need for electrically insulating coatings in contact with the flowing liquid metal.

To evaluate the coating concept, tests were conducted at Argonne National Laboratory to evaluate the MHD performance of electrical insulator coatings that use a eutectic liquid metal of composition Na-78 wt.% K (NaK).[3] Aluminum oxide was chosen as the candidate insulating material for the proof-of-concept because it is thermodynamically stable in NaK. A round pipe of type 304 stainless steel was aluminized on its inside surface by a pack-diffusion method, in which the substrate material is contacted and heated for 4-12 h at ≈900°C with a pack of powders. The composition of such powders (e.g., 65 wt.% Al_2O_3, 33 wt.% Al, 2 wt.% NH_4Cl) provides metallic Al, alumina as filler material, and NH_4Cl as activator. The Al deposited on the substrate surface diffuses into the subsurface regions of the material, where it forms intermetallic phases as aluminides of Fe and/or Ni. Because the substrate materials are heated to temperatures close to the annealing range for times sufficient to cause solution processes in the matrix, they generally need a final treatment to optimize the structure. The aluminide layers reached thicknesses of 0.025-0.20 mm, depending on the exposure time and temperature and composition of the substrate material. The aluminum concentration reached 50 wt.% or more over a depth of ≈160 μm from the surface, beyond which it decreased to zero at a depth of ≈440 μm.

After aluminizing by the above procedure, the pipe required oxidizing at elevated temperature for a time sufficient to develop an adherent alumina layer with adequate insulating properties. Based on the laboratory tests on oxidation of aluminized specimens, an oxidation period of 4 h at 982°C was selected for oxidation of the aluminized pipe. The alumina-coated 304 stainless steel pipe was used a test section in MHD pressure-drop tests conducted over a 0-20 T range of magnetic field strength and an average NaK velocity of ≈6.5 cm/s at bulk fluid temperatures of 30 and 85°C. The overall pressure drop across the entire magnet was determined by measuring the differential pressure between pressure taps located at each end of the test section. Test results showed that the pressure drop with an insulator coating was 25 times lower than that obtained on an uncoated tube under identical test conditions. The measured values for the insulated pipe were somewhat higher than that calculated for a perfectly insulated pipe, and possible causes for this difference are discussed elsewhere.[3]

The electrical insulating coating for service in an Li (the candidate coolant for fusion system) environment must not only have adequate electrical resistivity over a wide range of temperature but also

be compatible with Li and be capable of self healing, if defects develop in the coating during service. A review of available information on the electrical resistivity values for several oxides, nitrides, and mixed oxides showed that oxides such as CaO, MgO, BeO, Y_2O_3, and $MgAl_2O_4$, and nitrides such as BN, AlN, and Si_3N_4 exhibit resistivities of $>10^6$ Ω·cm at temperatures below $\approx$700°C (see Fig. 1). The requirement is that the product of the electrical resistivity of the insulator coating and the thickness of the coating should exceed a nominal value of 100 Ω·cm^2 under operating conditions. This translates to a minimum resistivity value of 10^6 Ω·cm for a coating thickness of 1 μm, or 10^5 Ω·cm for a coating thickness of 10 μm. Based on the resistivity values of materials listed above, a coating layer of <1 μm in thickness of any of these materials would be adequate from the insulating standpoint, provided that resistivity is not reduced during operation, e.g., by irradiation.

Figure 2 shows the thermodynamic stability of several oxides (CaO, MgO, Y_2O_3, BeO) that are possible candidates for insulator application in an Li environment. It is evident that all four oxides are stable in O-saturated Li at temperatures of >200°C. Also shown in the figure are free-energy values for Li that contains various concentrations (1000, 300, 100, and 38 wppm) of O. The lowest value of 38 wppm O corresponds to an O concentration that is established by cold-trapping Li at 200°C. Under these conditions, only BeO and CaO are thermodynamically stable over the wide temperature range (200-700°C) of interest for fusion systems, but MgO and Y_2O_3 will be reduced to metal by Li at temperatures > 460°C. Furthermore, based on the binary Li-Ca phase diagram, a significant amount of Ca can be dissolved in Li at fairly low temperatures, and this feature may aid in development of in-situ CaO coatings and also enable self-healing for the defects, if any, in the coatings by transport of Ca to the defect region and subsequent oxidation. Based on this analysis, CaO was selected as an insulator candidate for evaluation in Li systems.

Figure 3 depicts the thermodynamic stability of nitrides of several structural metals with respect to N concentration in an Li environment. The data indicate that compounds such as BN and AlN, which possess high resistivity, will be stable over a wide temperature range in an Li environment even with N concentrations as low as 100 wppm. Si_3N_4 is marginally stable in Li, while TiN, even though stable, has low resistivity. Furthermore, Li has a fairly high solubility for Al and N, and this characteristic (similar to that for Ca) can enable self-healing of defects by providing flexibility in the control and maintenance of chemistry of Li. Among the nitrides, AlN was selected as a possible coating for V-Li blanket applications.

Development of Coatings for Use in Li environment

CaO coatings were developed by vapor phase transport, in which V-alloy specimens were exposed to a pack of fine Ca pellets at 700-800°C in a static Ar environment. Figure 4 shows the temperature dependence of the vapor pressure of Ca. Above 700°C, the vapor pressure of Ca is >0.1 torr, sufficient to deposit a layer of Ca on the specimens. The exposure time in the deposition process ranged from 100 to 200 h. Upon deposition of Ca, the specimens were oxidized in an Ar environment to oxidize the Ca deposit. The oxidized specimens exhibited poor adherence of the oxide to the substrate, and the oxide layer was patchy and fairly thin. The patches of coatings exhibited insulating characteristics after this oxidation step. X-ray diffraction studies on these specimens showed good correlation between high resistance values at room temperature and a high concentration of Ca in oxide form. Calcium concentrations of 60-80 wt.% were obtained in several specimens. However, coating thickness in a given specimen or among various specimens was not uniform; in some specimens, coating spallation was noted. The results also showed that Ca deposition via vapor phase transport is possible but that the

coating thickness and the adhesive bonding of the coating to the substrate after a single deposition/oxidation procedure were not adequate to produce the desired insulating characteristics. Additional experiments, with several procedural modifications, were conducted and, finally, a double deposition/oxidation treatment seemed to produce a thicker coating that was more adherent and exhibited adequate insulating characteristics.

Figure 5 shows typical SEM photomicrographs of cross sections of two V-4Cr-4Ti alloy specimens after a double Ca deposition/oxidation treatment. EDX analysis of the specimen surfaces showed the coatings to be CaO and also revealed the virtual absence of any elements from the substrate alloy. Depth profiles for two of the coated specimens are shown in Fig. 6; the profiles indicate coating thicknesses of 16 and 34 μm, respectively. The difference in scale thickness between the two specimens in due to the proximity of different specimens to the Ca pack. Resistance measurements were also made on specimens that were double Ca/oxidation treated and subsequently exposed to liquid Li of normal purity at 500°C for 68 h. Figure 7 shows the variation in the product of resistance times area (i.e., R x A, which is equivalent to the product of resistivity times coating thickness) as a function of temperature obtained on a CaO-coated and Li-exposed specimen of V-4Cr-4Ti alloy. The figure shows that R x A values are $>10^7$ $\Omega \cdot cm^2$ from room temperature to 200°C; the value gradually decreases to $\approx 5 \times 10^6$ $\Omega \cdot cm^2$ as temperature is increased from 200 to 540°C. The specimen was maintained isothermally at ≈540°C for ≈6 h, after which it was further heated to ≈700°C. Even at 700°C, the specimen exhibited an R x A value of 10^4 $\Omega \cdot cm^2$, at least two orders of magnitude higher than that required in a fusion device using a Li blanket.

PVD was used for development of AlN coatings on both bare and prealuminized V-5Cr-5Ti alloy. Aluminum nitride was sputter-deposited reactively. That is, an aluminum target was sputtered in a partial pressure of high-purity nitrogen, with argon as the primary sputtering gas. Because the process takes place in a vacuum chamber and uses high-purity reactants, the coating product should also be very pure. The process takes place at a relatively low temperature, generally not above ≈250°C. The chamber was initially pumped down to 2×10^{-6} torr before coating began. Specimens of both bare and prealuminized V-5Cr-5Ti and the Al target were sputter-cleaned for 6 min with high-purity argon at a flow rate of 45 cm^3/min and a chamber pressure of 20 mtorr. Subsequently, AlN_X was sputter-deposited with a 1200 W RF power source for 10 h in an argon-nitrogen gas mixture at a chamber pressure of 23 mtorr. The sputtered specimens were cooled in vacuum overnight, and the second side of the specimens was then coated the same way. X-ray diffraction analysis of the coated specimens showed hexagonal AlN phase with (002) orientation.

Figure 8 is an SEM photomicrograph in cross section of an AlN-coated V-5Cr-5Ti alloy specimen after 430 h exposure at 300°C to an Li environment in which argon-nitrogen gas was bubbled for 24 h. Figure 9 shows EDX depth profiles for Al, N, V, Cr, and Ti, AlN-coated, prealuminized V-5Cr-5Ti alloy specimen after similar exposure to Li. The concentration profiles show that the coating is predominantly Al and N, with almost no contamination from either the impurities in Li or the substrate constituents. Resistance measurements were made on bulk AlN samples and AlN coatings developed by PVD, after exposure in an Li environment at 300°C. Figure 10 shows the variation in R x A as a function of temperature for the bulk AlN specimen after exposure in an Li environment at 300°C. The value for R x A is $>10^7$ $\Omega \cdot cm^2$ at temperatures up to ≈300°C, beyond which the resistance decreases but still has a value of 10^4 $\Omega \cdot cm^2$ at a temperature up to 700°C. Results indicate that a fairly constant value of resistance is observed at each temperature used for the isothermal evaluation and that the values are substantially higher than needed for blanket application.

Coatings for Sulfur Resistance

Earlier studies of high-temperature corrosion of conventional engineering alloys and advanced nickel- and cobalt-base alloys showed significant sulfidation attack in environments with the low oxygen partial pressures (pO_2) and moderate-to-high sulfur partial pressures (pS_2) that are typical of coal gasification and substoichiometric combustion systems.[4-7] In these studies, extensive analyses were performed on the scales on several advanced alloys after exposure to simulated mixed–gas atmospheres; the reaction models were used to explain the behavior of these materials in the different regimes defined by the temperature and oxidant (O_2 and S_2) partial pressures. Improvements in corrosion resistance were also sought in a number of research programs to use the materials under lower pO_2 and higher pS_2 conditions and to prolong alloy performance before breakaway (accelerated) corrosion occurs.

Because the major objective in the development of corrosion- (sulfidation-) resistant alloys is formation of a slow-growing scale that is well bonded to the substrate alloy, research is underway to modify the surface regions of the alloy in order to enhance nucleation/growth of the oxide scale in the early stages of alloy exposure. The modifications produce both physical changes (e.g., grain size) and chemical changes (e.g., composition, grain boundary segregation, creation of metastable phases). One way to improve corrosion resistance of structural alloys is to apply a coating that is resistant to chemical and physical interactions with the hostile environment. In general, coating systems can be classified as either diffusion or overlay types; these are distinguished principally by deposition method and resulting coating/substrate bond structure. Among the numerous coating techniques, weld overlay, pack diffusion, and ESD processes have been examined for applications in heat recovery units of coal conversion systems. In addition, plasma spray in either reduced pressure or vacuum and ESD techniques have been examined for improved erosion/corrosion resistance in gas turbine applications in combined-cycle plants.

A number of different coatings (see Table 2) were applied on T22 substrate alloy by both pack diffusion and ESD.[8] Of the nine coatings on T22 substrate, six were exposed for 2000 h to a gas mixture with a low- pO_2 and high pS_2 at 500 and 650°C. Figure 11 shows SEM photomicrographs of corrosion scale morphologies observed on different coatings subsequent to exposure at 500°C. The chromized, aluminized, and simultaneously chromized/aluminized coatings exhibit a substantial decrease in sulfidation attack and metal wastage via corrosion when compared with the uncoated T22 alloy. On the other hand, specimens with XF2020 coating (Fe–20Mo–20Cr–10Ni) with or without a refractory-metal bond coat developed iron sulfide scales that adhered to the substrate but were almost as thick as in the uncoated T22 alloy. The Fe_3Al coating, with or without Nb-1Zr bond coat, exposed for 500 h also exhibited iron sulfide scales of substantial thickness. A specimen with a chromized coating developed a thin Cr sulfide scale with a thickness that was only about 20% of that of the chromized layer. A specimen with an aluminized coating exhibited a thinner scale that contained Fe, Al, and S. The specimen with a bond coat of Cr carbide developed a somewhat thicker Fe sulfide scale, and Al in the coating had no effect on morphology or scale thickness. The aluminized coating applied via ESD was much thinner (≈10 μm) than those applied with pack diffusion (≈200-400 μm), and these early coatings developed by ESD also exhibited dilution in Al concentration. The simultaneously chromized and aluminized specimen developed a thin (Fe,Cr) sulfide scale, but the zone underneath the scale was enriched in Cr and Al and had virtually no Fe. This zone seems to act as a barrier to outward Fe transport, thereby minimizing sulfidation attack. Figure 12 shows a comparison of the corrosion loss data obtained for T22 alloy in the uncoated condition and for several different coatings after exposure to gas mixture containing low- pO_2 and high pS_2 at 500 and 650°C. Similar corrosion loss data have been

reported for other test temperatures and for coatings developed on Fe-9Cr-1Mo steel.[8]

In recent years, Fe aluminide coatings have been developed by modifying the ESD procedure to minimize Al dilution in the coating.[9-11] Several specimens with Fe_3Al coating, applied on Type 316 stainless steel and Alloy 800 substrate alloys by the ESD, were tested in environments that contained low pO_2, moderate H_2S, and with or without HCl.[9] Figure 13 shows corrosion loss data obtained for specimens tested for 1000 h at 650°C in gas mixtures where $pO_2 = 1.2 \times 10^{-23}$, $pS_2 = 5.2 \times 10^{-10}$, $pCl_2 = 9.4 \times 10^{-17}$, and $pHCl = 2.1 \times 10^{-3}$ atm. All of the Fe aluminide coatings were resistant to sulfidation and chloride attack, whereas the base alloys were susceptible to general corrosion and pitting attack, especially in the HCl-containing environment. Weight change data and extensive microscopic analyses of tested specimens showed that the bond coats themselves do not significantly influence the corrosion process.

Further evaluation of Fe aluminide coatings was conducted with a Type 316 stainless steel substrate coated with FeAl welding rod.[10] Coatings made with FeAl welding rod contained much more Al than those made with Fe_3Al welding rod. Type 316 stainless steel specimens with and without coatings and several commercial high-Cr alloys were exposed to O/S mixed-gas environments for up to 728 h and periodically retrieved to measure weight changes at intermediate exposure times. Weight change data were obtained for several commercial high-Cr alloys exposed together with FeAl-coated Type 316 stainless steel in O/S mixed-gas environments with and without HCl. Figure 14 shows corrosion loss data based on parabolic kinetics for several of these alloys and coatings. The corrosion performance of the FeAl-coated specimen is comparable to or better than those of most other materials tested. Furthermore, the cost of materials such as HR 160 and Alloy 556, which exhibit corrosion rates similar to FeAl layered specimen, will be higher by a factor of 5 to 10 times than that of the FeAl-coated specimen.

Specimens with Al-enriched surfaces, applied on Type 316 stainless steel and Alloy 800 substrate alloys by the ESD process, were also tested in simulated combustion environments that contained SO_2 with or without HCl. Specimens were tested for ≈900 h at 650°C in gas mixtures with $pO_2 = 6.7 \times 10^{-3}$, $pS_2 = 1.5 \times 10^{-35}$, $pCl_2 = 3.6 \times 10^{-4}$, and $pHCl = 1.7 \times 10^{-3}$ atm. Figure 15 shows weight change data for Alloy 800 and Type 316 stainless steel and for Fe_3Al- or FeAl-coated Type 316 stainless steel as a function of exposure time at 650°C to simulated combustion environments with or without HCl. In the absence of HCl, the uncoated alloys developed scales of (Fe, Cr) oxide or Fe oxide and tended to crack and spall, as evidenced by weight loss. However, the absolute value for weight change after 900 h of exposure was <0.02 mg/mm^2. The aluminide-coated alloys showed a small weight gain due to the development of a thin, adherent alumina scale. In the presence of HCl, both the uncoated and coated alloys showed substantial weight loss at 650°C. The attack was most notable in the Fe_3Al-coated alloy, less notable in the uncoated alloys, and least notable in the FeAl-coated alloy.[11]

To examine the cause(s) for the increased corrosion of the Fe aluminide in HCl-containing environments, depth profiles for several of the pertinent elements in the scale were obtained by Auger analysis after sputtering the surfaces for various times.[12] When Cl is present in the exposure environment, several constituents of the coating and substrate alloy can react to form volatile chlorides an occurrence that can lead to loss of the oxide-forming elements. The thermodynamics of the reaction of metals such as Fe, Cr, Ni, and Al with either Cl_2 or HCl in the exposure environment at 650°C have been calculated. Similar calculations were performed to examine the reactions between oxides of these

elements and either Cl_2 or HCl. The results showed that the driving force for the reaction between Fe and Cl_2 or HCl is sufficiently high in the simulated combustion environment to form volatile $FeCl_3$. Similarly, the driving force for the reaction between Al and Cl_2 or HCl is sufficiently high in the simulated combustion environment to form volatile $AlCl_3$, Al_2Cl_6, and AlOCl phases. On the other hand, the calculations indicate that reactions between Fe_2O_3 and Cl_2 or HCl and between Al_2O_3 and Cl_2 or HCl are not favored at 650°C in the simulated combustion gas chemistries used in the present experiments. The results also indicate that to minimize the formation and escape of volatile chlorides of oxide-forming elements, the alloys must form the stable oxides early in the oxidation process, which is difficult, especially at lower temperatures.

Surface modifiaction by sputter deposition of Si or Si plus O or ion implantation of Nb has also been examined to improve the sulfidation resistance of Fe-Cr and Fe-Cr-Ni alloys. A deposit of Si or Si plus O results in formation of silicide phase on the surface, which eventually converts to silica during exposure in O/S mixed gas environments. Figure 16 shows the weight change data for Fe-25 wt.% Cr alloy with and without Si addition, after exposure in a mixed gas containing high H_2S at 700°C. It is evident that the corrosion rate (which is the slope of the weight change vs. time plot) decresed substantially in Si sputtered specimen. Furthermore, the presence of silica stabilizes chromia in the early stages of oxidation and minimizes iron transport outwards from bulk alloy. Ion implantation of Nb also improves the stabilization of chromia scale in the early stages of oxidation by enhancing the diffusion of Cr toward the surface. Figure 17 shows weight change data for Fe-25 wt.% Cr and Fe-25 wt.% Cr-20 wt.% Ni alloys with and without Nb implantation, after exposure in a mixed gas containing low H_2S at 700°C. At high H_2S levels, the benefit of Nb is much less in the Ni-containing alloy, indicating that at a given temperature a threshold H_2S level exists above which the resistance to sulfidation may not be sufficient. The scale developed with Si- or Nb-modified surfaces was protective against sulfur even under thermal cycling conditions.

Coatings for Hot Corrosion Resistance

Aluminide coatings developed by the pack-diffusion process have been used extensively as protection against hot corrosion of nickel- and cobalt-based superalloys in gas turbine applications. Corrosion of materials in the presence of liquid sodium sulfate, either by itself or in combination with sodium chloride, has been a problem in gas turbines; this corrosion process has been termed "hot corrosion" to differentiate it from gas-phase sulfidation attack. Two types of hot corrosion have been identified: Type I, operative at 800-950°C, and Type II, operative at 600-750°C.

Type I hot corrosion can be divided into an initiation (or incubation) stage and a propagation stage. The process, in general, requires the presence of liquid sodium sulfate (melting point 884°C) on the metal surface. In the initiation stage, the protective oxide scale dissolves by a basic fluxing mechanism and the corrosion rates are generally low. In the propagation stage, with the protective oxide having been destroyed and unable to reform, the alloy is subjected to sulfidation by inward diffusion of sulfur, leading to accelerated corrosion rates.

Type II hot corrosion, also known as low-temperature hot corrosion, involves the eutectics of base-metal sulfates and sodium sulfate and therefore occurs predominantly at lower temperatures, especially in turbines that operate in the effluent of FBCs. Protective coatings examined for hot-corrosion resistance are simple aluminides, precious-metal aluminides, and overlay-type coatings. The former two are made by the pack process, whereas in the overlay process, the coating elements are

applied directly onto the substrate by PVD or by the low-pressure plasma spray (LPPS) approach.

Figure 18 shows comparative data for corrosion of simple aluminides, aluminides with rhodium and platinum bond coats, and CoCrAlY overlay coating after exposure to a hot corrosion environment at 982°C.[13] Performance of a given coating is strongly influenced by the substrate alloy (more so in pack than in overlay coatings), and a bond coat of precious metal platinum (rather than rhodium) is beneficial in reducing corrosion in alloys such as IN 792 and IN 738. The overlay CoCrAlY coating on a cobalt-base MarM-509 alloy exhibited the best performance among all the coatings examined in this study. Extensive microstructural analyses of the tested coatings have been reported[13] and qualitative inferences have been drawn from the test results, but a discussion of those results is beyond the scope of this paper. Corrosion test data obtained in the effluent of a pressurized FBC system showed that both nickel– and cobalt–base alloys were equally susceptible to accelerated corrosion. This susceptibility to accelerated corrosion was attributed to the presence of potassium in the FBC effluent.[14] Information on the performance of coating/substrate combinations under low–temperature hot-corrosion conditions is particularly lacking at present. Another study conducted to evaluate the performance of different coatings and coating methods on a given alloy substrate showed that the LPPS overlay of CoCrAlY, especially the high-chromium version, exhibited the longest life when compared with electron-beam overlay of CoCrAlY, precious metal aluminides, and simple aluminides (see Fig. 18).[15]

Summary

Surface modification is an approach that is widely used to achieve several objectives such as meeting functional requirements, minimizing wastage and costs, and protecting downstream components. This paper addresses several advantages for the use of surface modification approaches and identifies several criteria for selecting and applying modified surfaces in the power generating sector. Brief discussions on several surface modification techniques are presented, with the emphasis on coatings. Finally, the paper discusses in detail the application of electrically insulating functional coatings in the first-wall blanket of a fusion device, coatings for sulfur resistance in fossil systems, and functional, hot-corrosion-resistant coatings for use in gas turbines.

Acknowledgments

This work was supported by the U.S. Department of Energy, Office of Fossil Energy, Advanced Research and Technology Development Materials Program and Office of Fusion Science, under Contract W-31-109-Eng-38. D. L. Rink assisted with several aspects of the experimental program.

References

1. S. Malang, H. U. Borgstedt, E. H. Farnum, K. Natesan, and I. V. Vitkovski, "Development of insulating coatings for liquid metal blankets," Fusion Engineering and Design, 27 (1995) 570-586.

2. S. Malang and L. Bühler, "MHD pressure drop in ducts with imperfectly insulating coatings," Argonne National Laboratory Report ANL/FPP/TM-269 (August 1994).

3. C. B. Reed, K. Natesan, T. Q. Hua, I. R. Kirillov, I. V. Vitkovski, and A. Anisimov, "Experimental and theoretical MHD performance of a round pipe with a NaK-compatible Al_2O_3 coating," Proc.

3rd Intl. Symp. on Fusion Nuclear Technology, Los Angeles, June 27-July 1, 1994, Fusion Engineering and Design, 27 (1995) 614-626.

4. K. Natesan, Corrosion and Mechanical Behavior of Materials for Coal Gasification Applications, Argonne National Laboratory Report ANL–80–5 (May 1980).

5. T. C. Tiearney, Jr., and K. Natesan, Oxid. Met., 17 (1982) 1.

6. K. Natesan, in M. A. Dayananda, S. J. Rothman, and W. E. King (eds.), Symposium on Oxidation of Metals and Associated Mass Transport, TMS–AIME, 1987, p. 161.

7. K. Natesan, in W. T. Bakker, S. Dapkunas, and V. Hill (eds.), Proc. Conf. Materials for Coal Gasification, ASM International, 1987, p. 51.

8. K. Natesan and R. N. Johnson, Surface and Coatings Technol., 43/44, 821, 1990.

9. K. Natesan and R. N. Johnson, Proc. 2nd Int. Conf. on Heat Resistant Materials, Gatlinburg, TN, Sept. 11-14, 1995, ASM International, Materials Park, OH, 1995, p.591.

10. K. Natesan, Proc. 11th Annual Conf. on Fossil Energy Materials, ORNL/FMP-97/1 (1997) p. 289.

11. K. Natesan and P. F. Tortorelli, Proc. Int. Symp. on Nickel and Iron Aluminides: Processing, Properties, and Applications, Cincinnati, Oct. 7-9, 1996, ASM International, Materials Park, OH, 1997, p. 265.

12. K. Natesan, Proc. 12th Annual Conf. on Fossil Energy Materials, ORNL/FMP-98/1 (1998) p. 271.

13. F. S. Kemp, Electric Power Research Institute Report EPRI AP–1369 (1980).

14. R. W. Haskell, H. von E. Doering, O. H. Le Blanc, and K. L. Luthra, Final Report ORNL/Sub/84–00224/01 (1987).

15. S. Shankar, D. E. Koenig, and L. E. Dardi, J. Met., **33**, 13, 1981.

Table 1. Technical/economic factors in application of coatings

Cost comparison with monolithic but expensive material
Cost comparison with cladding and/or coextruded materials
Chemical compatibility with environment
Chemical compatibility with substrate
Coating/substrate interactions over time
Ease of application/coating integrity/reproducibility
Joining of coated components
Thermal compatibility
Feasibility of repair/recoating in field
Replacement cost and downtime expense
Initial cost outlay

Table 2. Details on alloy/coatings used in corrosion studies

Alloy/Coating	Composition	Coating Method
T22	Fe-2 1/4Cr-1Mo	-
T91	Fe-9Cr-1Mo	-
Alloy 800	Fe-32.5Ni-21Cr	-
310 SS	Fe-25Cr-20Ni	-
CR35A	45Ni–37Cr–Fe	-
CR30A	51Ni–31Cr–2Mo–Fe	-
T22/Fe_3Al	T22/Fe-15Al	ESD
T22/Nb-1Zr/Fe_3Al	T22/Nb-1Zr/Fe–15Al	ESD
T22/XF2020	T22/Fe-20Mo-20Cr-10Ni	ESD
T22/KBI10/XF2020	T22/Ta-10W/XF2020	ESD
T22/KBI41/XF2020	T22/Ta-37.5Nb-2.5W/XF2020	ESD
T22/C 815/Al	T22/Cr Carbide/Al	ESD
T22/Chromized	T22/Cr	Pack Diffusion
T22/Aluminized	T22/Al	Pack Diffusion
T22/Cr/Al	T22/Cr+Al	Pack Diffusion
T91/Chromized	T91/Cr	Pack Diffusion
T91/Aluminized	T91/Al	Pack Diffusion
T91/Cr/Al	T91/Cr+Al	Pack Diffusion

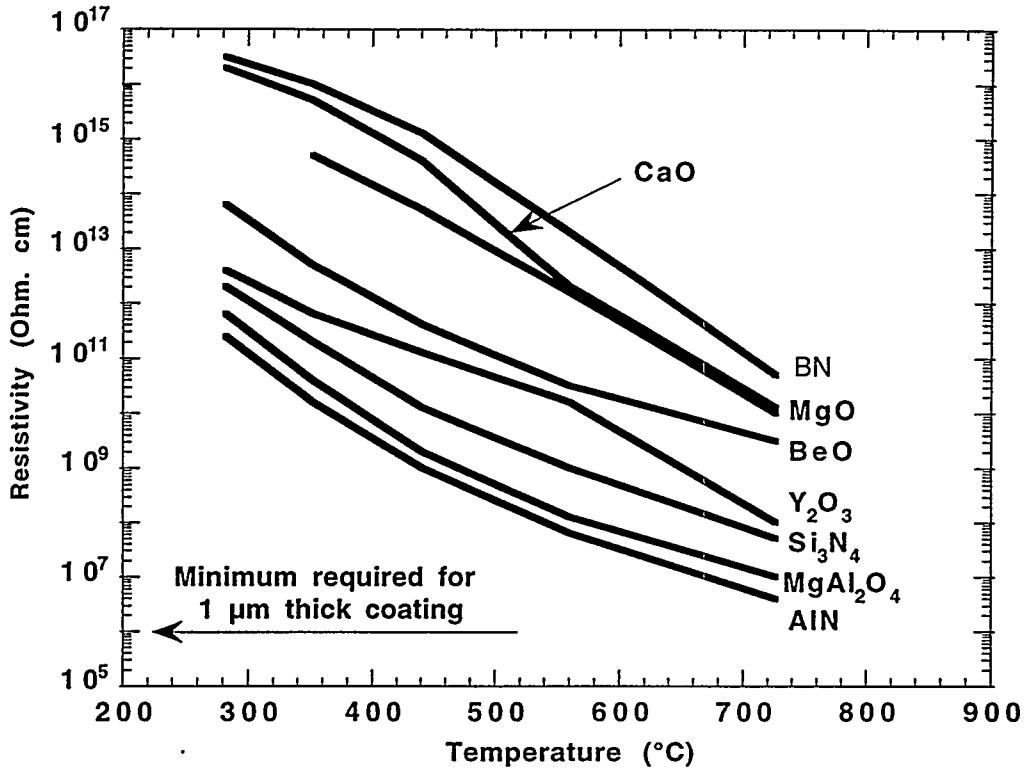

Fig. 1. Temperature dependence of electrical resistivity of several oxides and nitrides

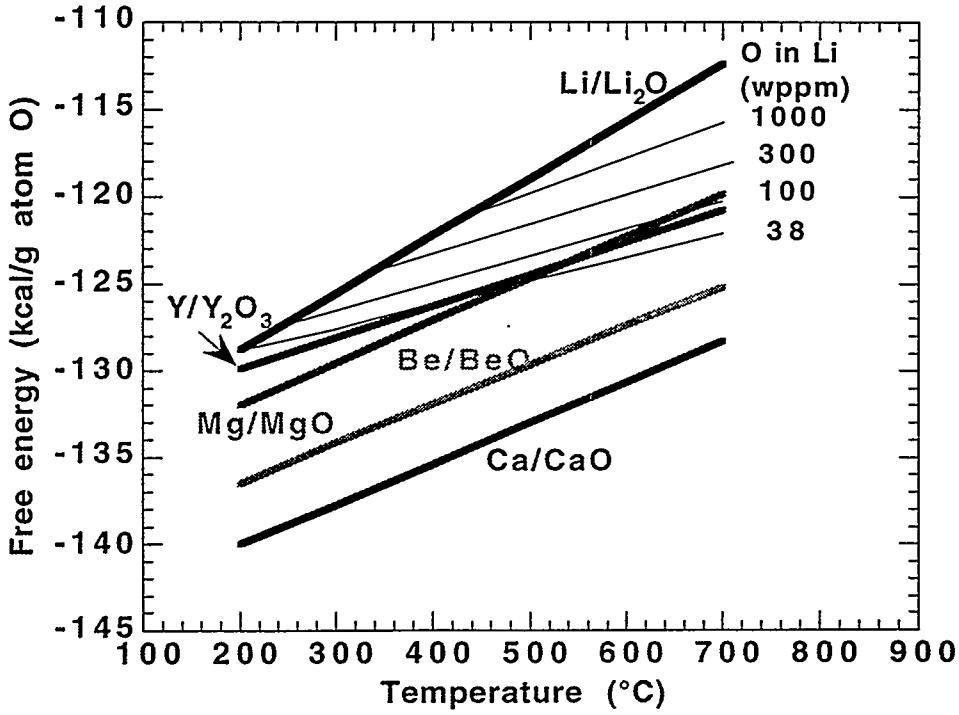

Fig. 2. Thermodynamic stability of candidate oxide coatings in an Li environment

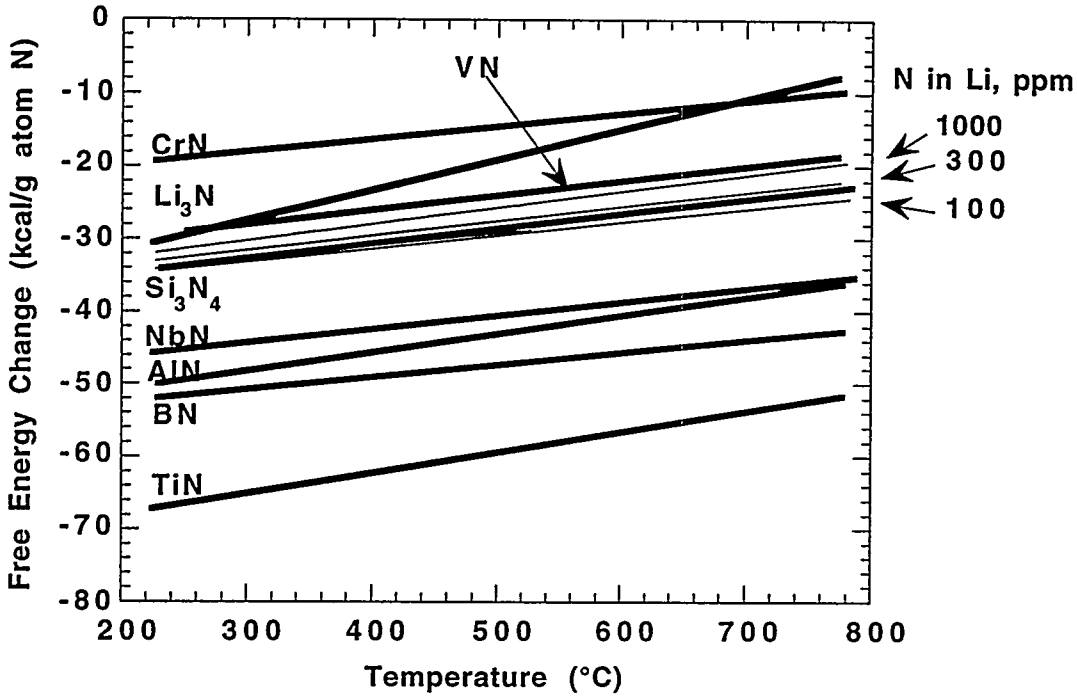

Fig. 3 Thermodynamic stability of several nitrides in an Li environment

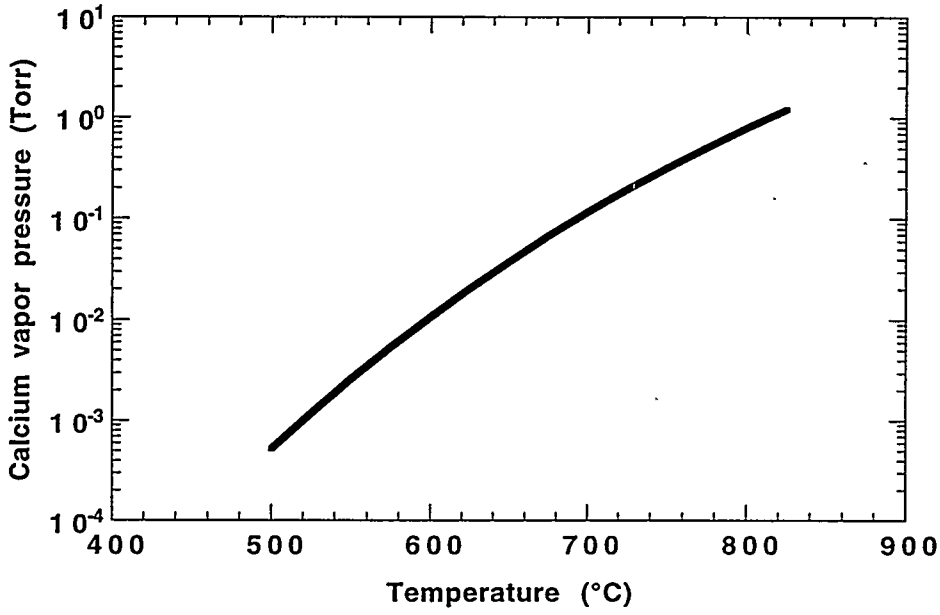

Fig. 4. Temperature dependence of vapor pressure of Ca

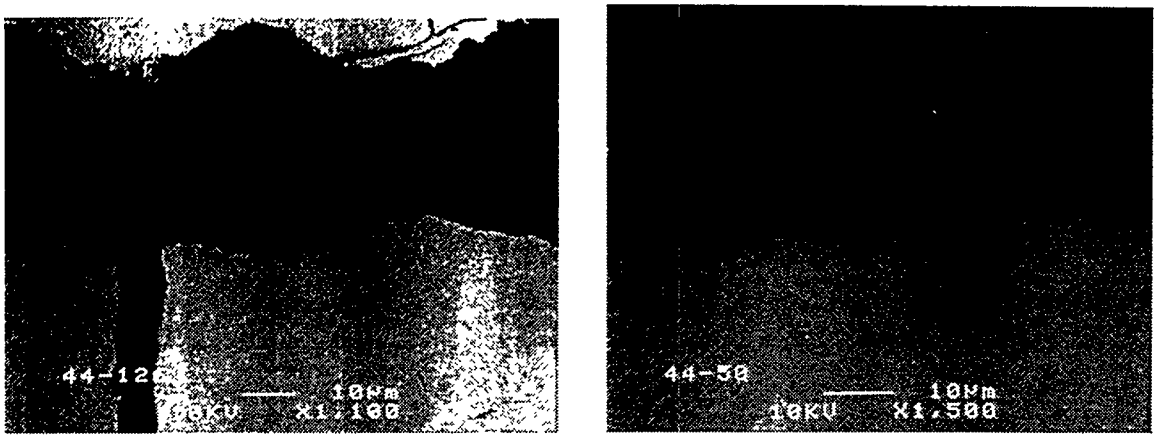

Fig. 5. SEM photomicrographs of cross sections of two V-4Cr-4Ti alloy specimens after double Ca deposition/oxidation treatment.

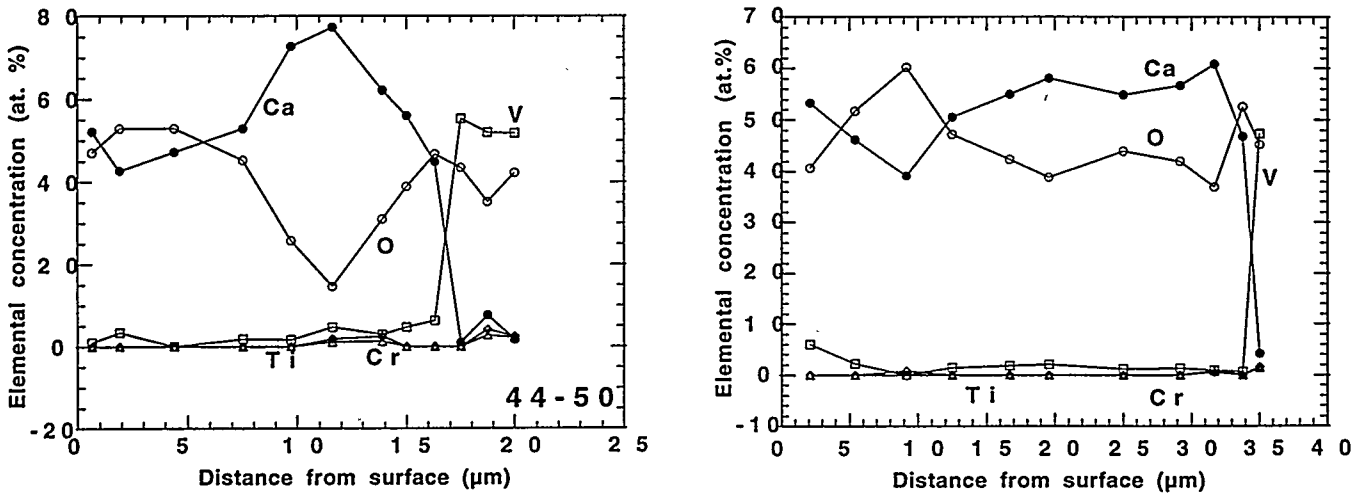

Fig. 6. Elemental concentrations as a function of coating thickness for V-4Cr-4Ti alloy specimens after double Ca deposition/oxidation treatment: coating thickness (left)16 μm; (right) 34 μm

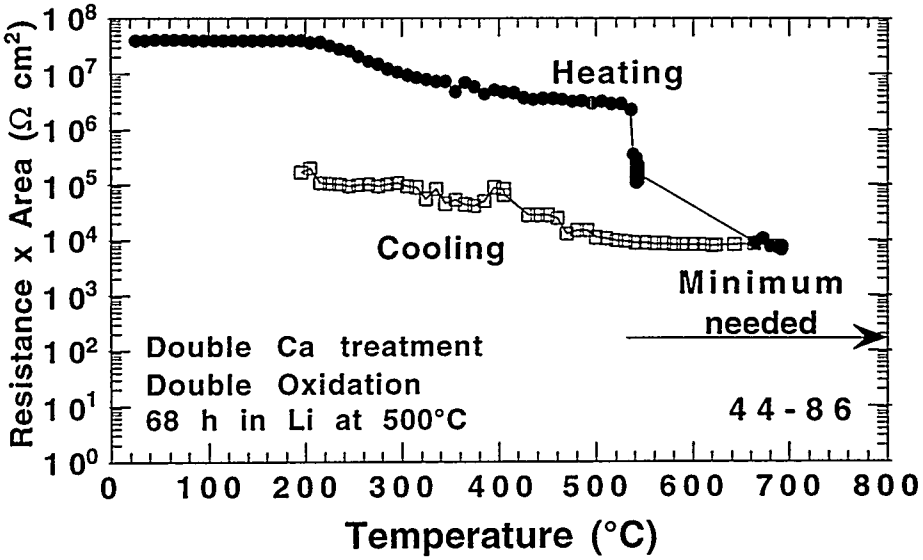

Fig. 7. Product of resistance times area as a function of temperature for V-4Cr-4Ti alloy with double Ca deposition/oxidation after 68-h exposure in Li environment at 500°C.

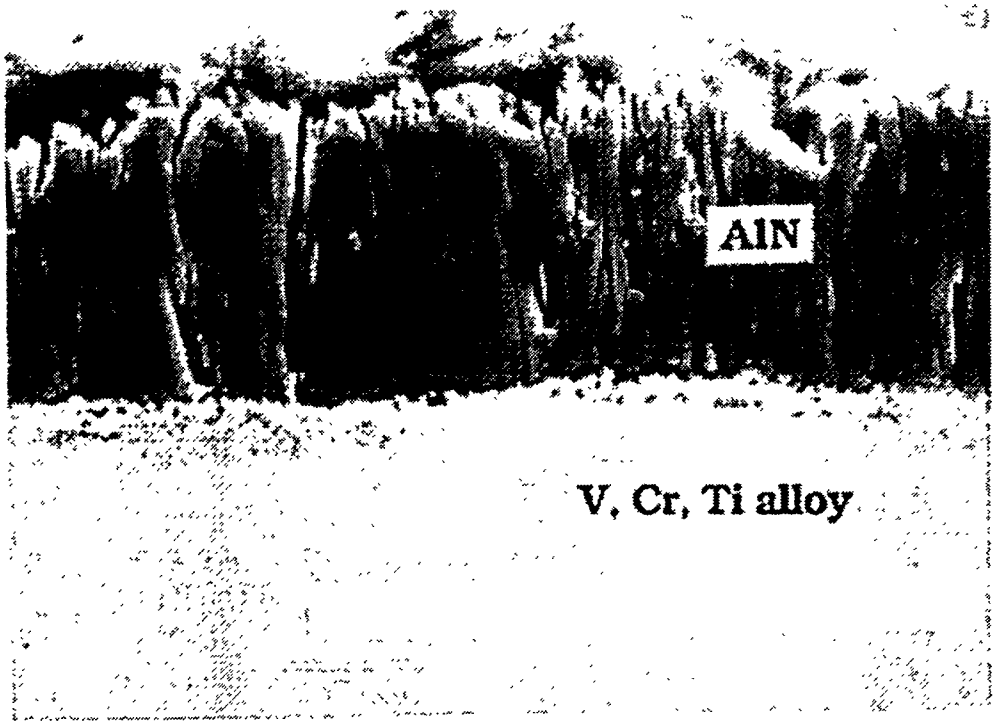

Fig. 8. SEM photomicrograph in cross section of AlN-coated V-5Cr-5Ti alloy specimen after 430 h exposure to Li environment at 300°C

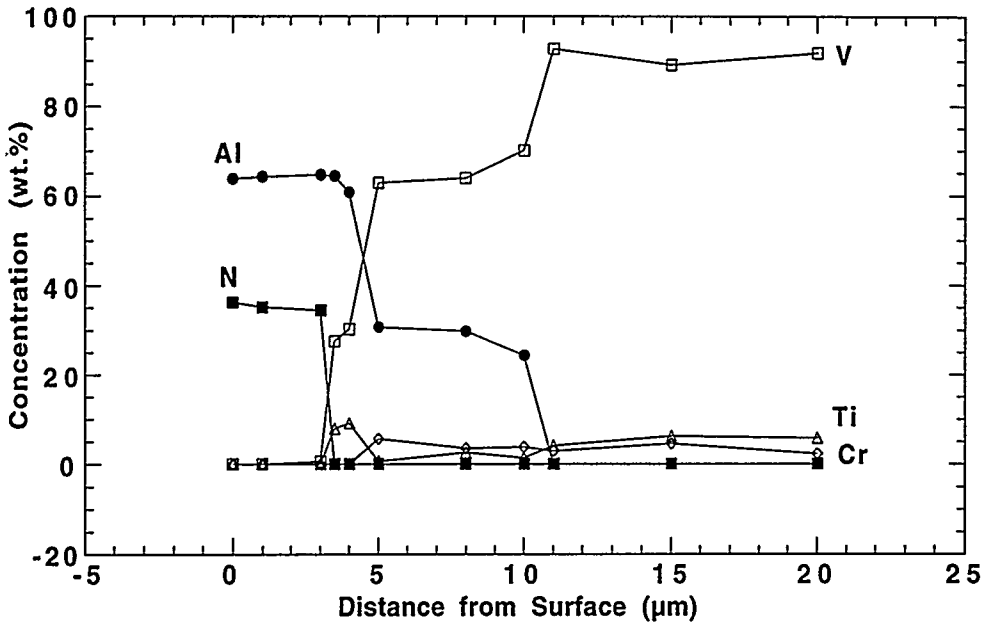

Fig. 9. EDX depth profiles for Al, N, V, Cr, and Ti for a V-5Cr-5Ti alloy specimen after 430 h exposure to Li environment at 300°C

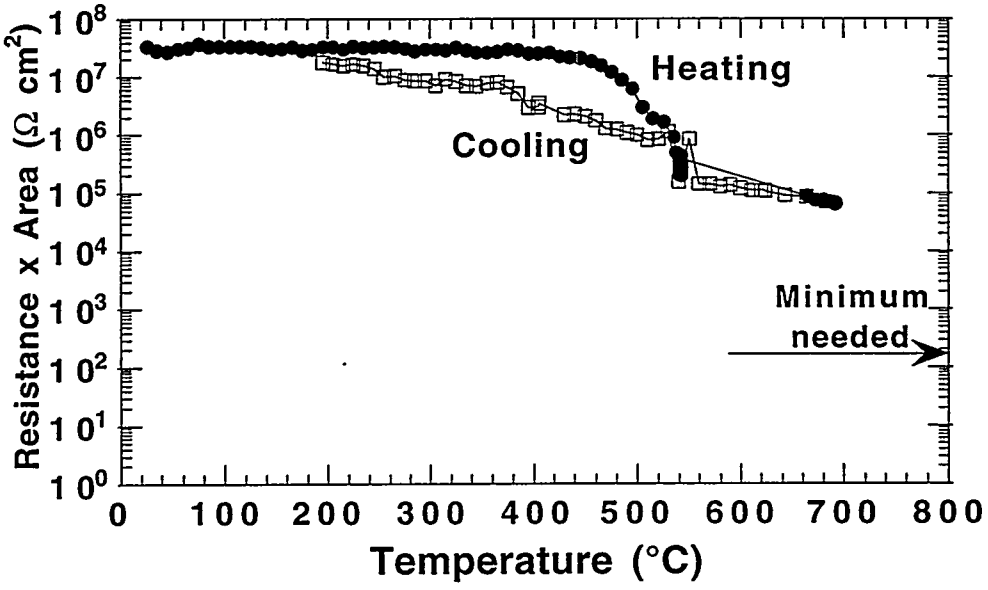

Fig. 10. Product of resistance times area as a function of temperature for V-5Cr-5Ti alloy with AlN coating developed by PVD, after exposure in Li environment

Fig. 11. SEM micrographs of uncoated and coated T22 alloys after 2000 h exposure to O/S mixed-gas environment at 500°C

Fig. 12. Corrosion loss data for T22 alloy in uncoated condition and with several coatings after 2000 h (unless marked otherwise) exposure to O/S mixed-gas environment at (a) 500°C and (b) 650°C

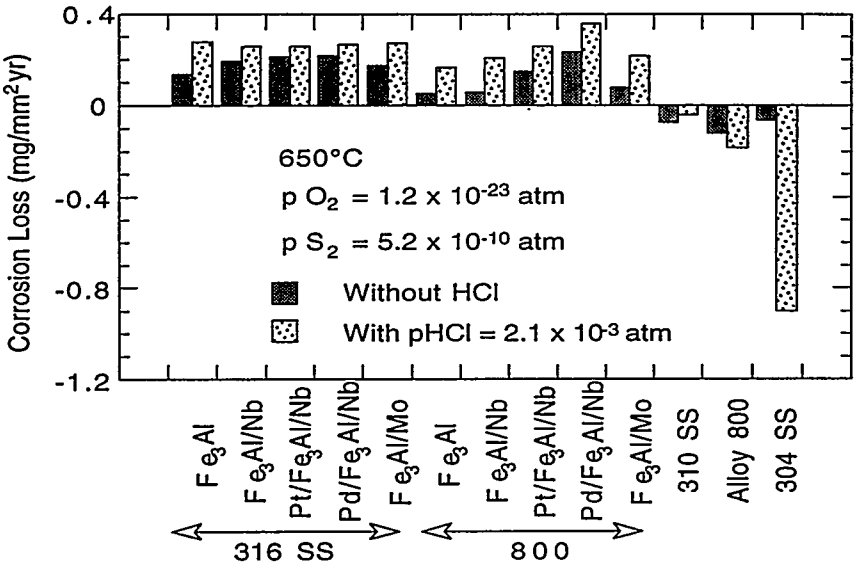

Figure 13. Corrosion loss data for several Fe_3Al coatings and uncoated austenitic alloys after exposure in gas mixtures containing H_2S with and without HCl.

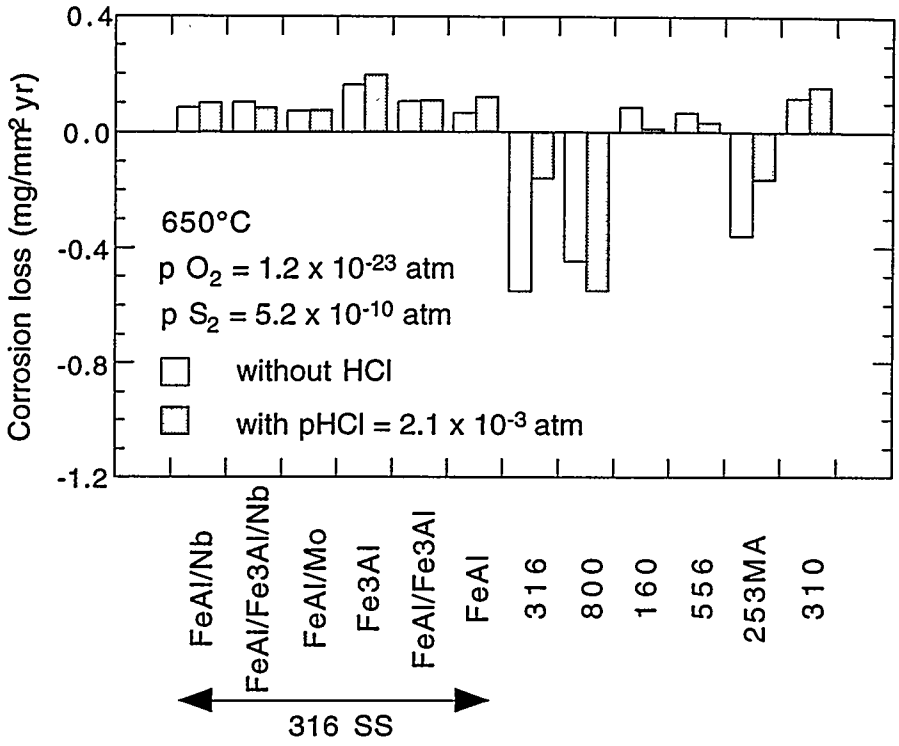

Figure 14. Corrosion loss data for FeAl coatings on Type 316 stainless steel and several uncoated high-Cr alloys after exposure in gas mixtures containing H_2S with and without HCl.

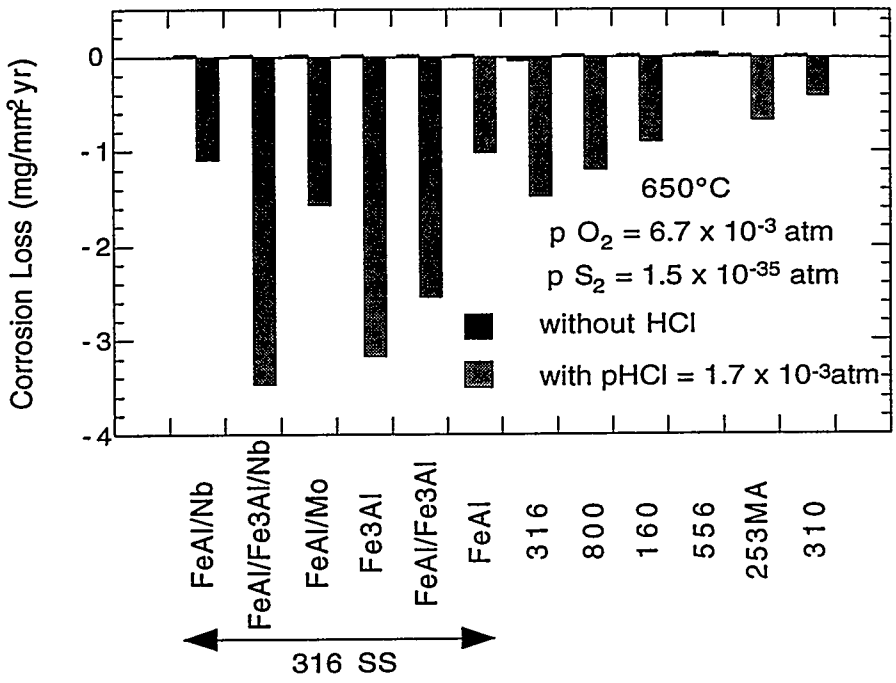

Figure 15. Corrosion loss data for Fe-Al coatings on Type 316 stainless steel and several uncoated high-Cr alloys after exposure in gas mixtures that contained SO_2 with and without HCl.

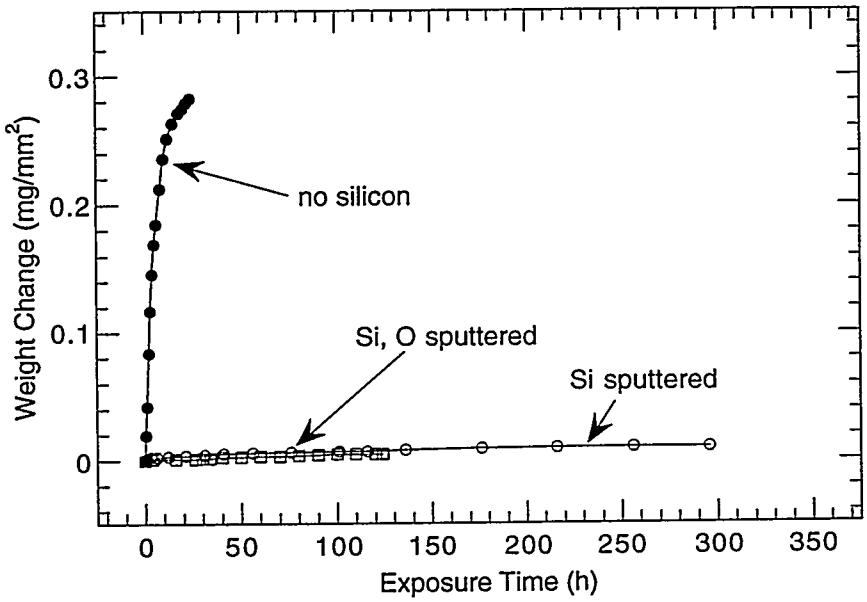

Figure 16. Weight change data for Fe-25 wt.% Cr alloy with or without Si and/or Si plus O sputter deposit after exposure to O/S mixed-gas environment at 700°C

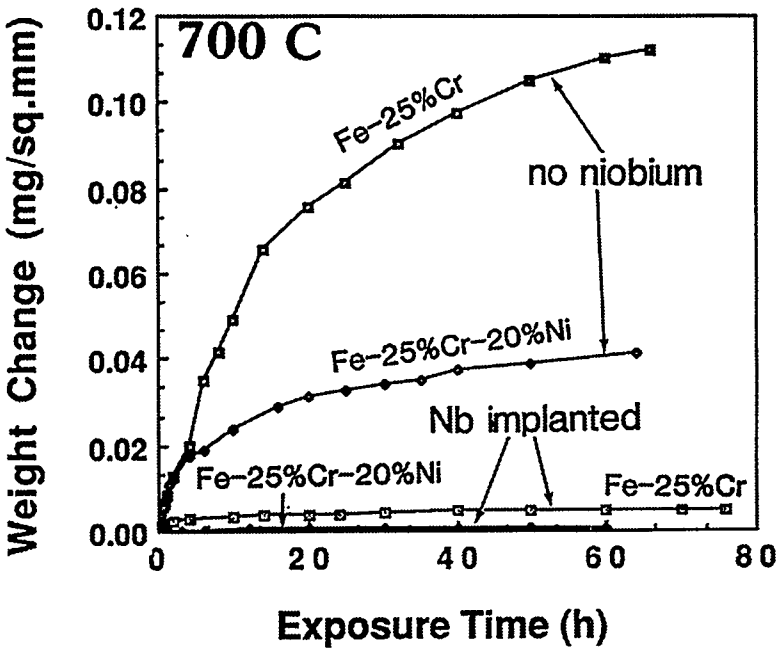

Figure 17. Weight change data for Fe-25 wt.% Cr and Fe-25 wt.% Cr-20 wt.% Ni alloys with or without Nb implantation after exposure to O/S mixed-gas environment at 700°C

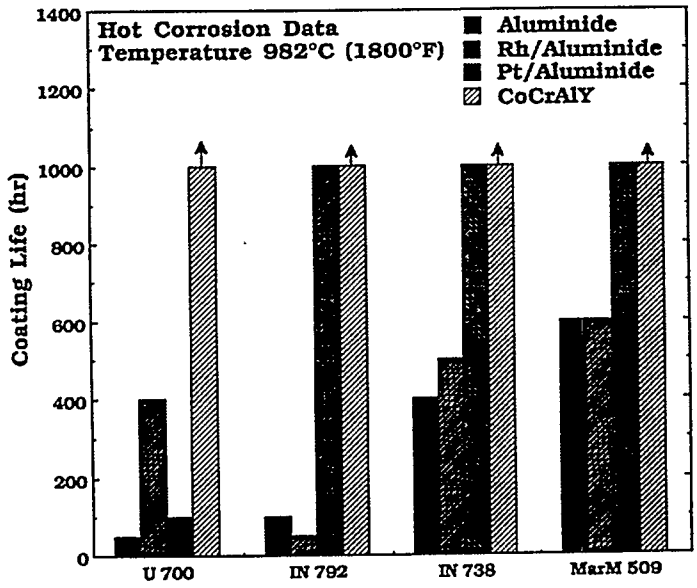

Figure 18. Coating life for several aluminide, precious-metal aluminide, and overlay coatings on nickel- and cobalt-base alloys exposed to hot corrosion environments.

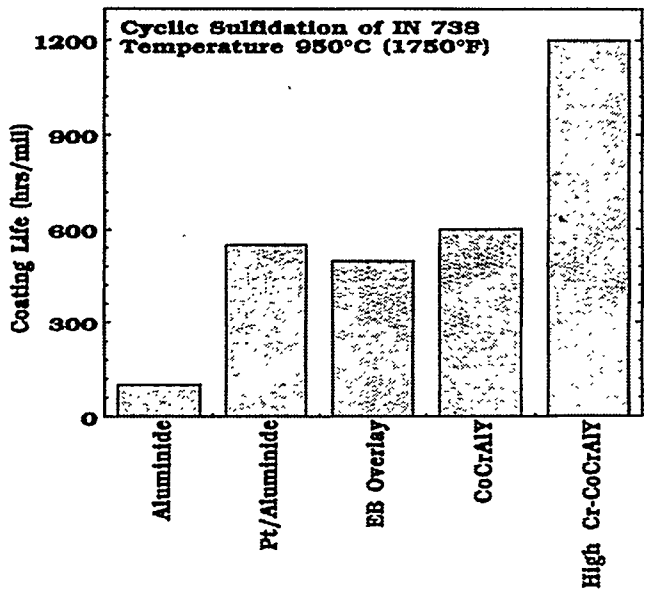

Figure 19. Ccoating life for several coatings on IN 738 exposed to hot corrosion conditions.